Stark effect in type-II Ge/Si quantum dots

A. I. Yakimov,* A. V. Dvurechenskii, A. I. Nikiforov, V. V. Ulyanov, A. G. Milekhin, and A. O. Govorov
Institute of Semiconductor Physics, Siberian Branch of the Russian Academy of Sciences, 630090 Novosibirsk, Russia

S. Schulze and D. R. T. Zahn
Institut für Physik, Technische Universität Chemnitz, D-09107, Chemnitz, Germany

(Received 12 September 2002; revised manuscript received 26 November 2002; published 31 March 2003)

Photocurrent spectroscopy was employed to study interband optical transitions and the quantum-confined Stark effect in an array of Ge/Si self-assembled quantum dots. The mean diameter and height of the Ge nanoclusters are about 6 nm and 4 nm, respectively. Under an applied electric field splitting of the exciton ground state is observed, implying that the dots possess two permanent dipole moments of opposite sign. We argue that the two possible orientations of the electron-hole dipole in each Ge dot are the result of the spatial separation of electrons which can be excited in Si as well as on top and below the Ge nanocluster. The separation of electron and hole is determined to be (5.1 ± 0.2) nm for the top (apex) electron and (0.8 ± 0.3) nm for the bottom (base) electron, yielding a distance between the electrons of (5.9 ± 0.5) nm, which is consistent with the staggered band lineup inherent to type-II quantum dots. An external quantum efficiency of 1% at a telecommunication wavelength 1.3 μm was obtained for a p-i-n structure.

DOI: 10.1103/PhysRevB.67.125318 PACS number(s): 78.67.Hc, 71.35.−y, 78.66.Db

I. INTRODUCTION

Zero-dimensional semiconductor structures [quantum dots (QD's)] display many effects known from atomic physics. One of such exciting phenomena is the redshift of the optical transition induced by an electric field [so-called quantum-confined Stark effect (QCSE)]. Recent theoretical[1–4] and experimental studies[5–8] reported for type-I InAs/GaAs and InGaAs/GaAs QD's, wherein the narrow-gap dot material presents a potential well for both electron and hole, demonstrated that the Stark shift can provide very useful information on the polarity of intra- and interdot electron-hole alignment and the vertical separation.

The change of the potential energy of a dipole with a moment $\mathbf{p}$ in an electric field $\mathbf{F}$ is given by $U = -\mathbf{p}F$.[9] For the electron-hole system, $\mathbf{p} = e(\langle \mathbf{r}_h \rangle - \langle \mathbf{r}_e \rangle)$, where $\langle \mathbf{r}_{e,h} \rangle$ is the mean electron (hole) position. In type-II QD's, only one of the charge carriers is confined inside the dot whereas another carrier resides outside the dot. In contradistinction with the case of type-I QD's, one can expect that in such a system the Stark effect should be extremely large because of the permanent spatial separation of electron and hole and the presence of the built-in electron-hole dipole.[4] To date, most work in the field of QCSE has concentrated on InAs/GaAs QD's, and so far there has been no experiment investigating Stark effect in excitonic transitions of type-II QD's.

It is generally accepted that Ge/Si(001) quantum dots exhibit a type-II band lineup.[10–14] When an electron-hole pair is photoexcited, the hole is captured into the quantum well of the Ge dot and creates an attractive Coulomb potential, resulting in a binding of an electron in Si [Fig. 1(a)] at the Si/Ge interfaces and forming the spatially indirect excitons. In the present work we use photocurrent (PC) spectroscopy to study the effect of an electric field on the interband transitions in Ge/Si(001) quantum dots.

II. EXPERIMENT

For controlled tuning of the electric field, the Ge QD's are embedded in the intrinsic region of an Si p-i-n diode (p^+ region uppermost), allowing fields up to 90 kV/cm to be applied parallel to the growth direction z (applying a reverse bias to a p-i-n structure results in an electric field pointing from n^+ substrate to p^+ surface). The band profile under reverse bias condition is shown schematically in Fig. 1(b).

Ge/Si QD's, more suitable for the Stark spectroscopy, must meet the following conditions. First, the size of the dots

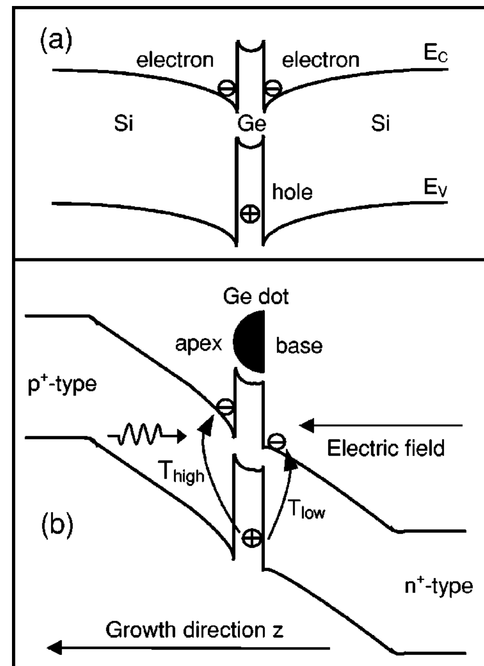

FIG. 1. (a) Band structure of the type-II Si/Ge/Si heterostructure along the growth direction through the center of the Ge dot. (b) Schematic band diagram of the p-i-n diode under reverse bias.

 ©2003 The American Physical Society

in all three dimensions should be small enough to provide actual zero-dimensional density of hole states. In this case, the localization of the hole in all three dimensions of Ge dot allows the electron in the Si conduction band to correlate more strongly with it, resulting in an increase of the exciton binding energy as compared with quantum-well systems.[15] Second, the electron and hole must be well separated to ensure the large dipole moment, so that the dots should be rather steep. However, conventional Ge/Si(001) self-assembled QD's, grown by Stranskii-Krastanov growth techniques, are always flat; i.e., they have an aspect ratio (height divided by base length) much less than unity.[16] To fabricate steep Ge islands with small lateral size, we grow the Ge dots on a Si(001) substrate covered with an ultrathin SiO_x film. Recently a similar approach has been successfully applied to form high-density ultrasmall Ge islands on Si(111) (Ref. 17) and Si(001) (Ref. 18) surfaces. The mechanism of Ge nanocluster formation on the ultrathin SiO_x films was essentially different from that on clean Si surfaces and is beyond the scope of this paper. A possible hypothesis has been put forward by Shklyaev and co-workers[17] and takes into account a reaction between individual Ge adatoms and SiO_x followed by a local silicon oxide desorption. The reflection high-energy electron diffraction (RHEED) data show that three-dimensional Ge islands are appeared without the preliminary formation of a wetting layer (no streaky RHEED pattern was observed beginning from the earliest stage of the Ge growth) and exhibit an epitaxial relationship with the underlying silicon substrate. The latter observation implies that, similar to the case of Stranski-Krastanov islands, Ge nanoclusters fabricated on an oxidized Si surface reside on *bare* Si regions.

The sample was grown by molecular-beam epitaxy at a temperature of 500 °C on an n^+-Si(001) substrate (7×10^{17} cm^{-3} As). The growth rates were 2 ML/s for Si and 0.2 ML/s for Ge. After preliminary chemical processing, the substrate was placed in the growth chamber where it was cleaned at 800 °C in a weak Si flux. As a result of the cleaning process, an atomically pure surface with a (2×1) superstructure is formed. For *p*-*i*-*n* structures 400-nm *i*-Si bottom region was first grown. To oxidize the surface, the oxygen had been introduced into the chamber at a pressure of 10^{-4} Pa for 10 min, which produces a SiO_x thickness of several Å. After oxygen was pumped out and the chamber pressure reached 10^{-7} Pa, nominally 1 nm of Ge was deposited. The growth of the QD's is followed by 400-nm *i*-Si and 200-nm p^+-doped Si layers (2×10^{18} cm^{-3} B). The structure was finally capped with a 10 nm of p^+-Si contact layer (10^{19} cm^{-3} B). The background boron concentration in the unintentionally doped *i*-Si layers was $(7-8)\times10^{15}$ cm^{-3}. Rectangular mesa diodes with areas ranging from 2.5×10^{-4} to 5×10^{-3} cm^2 were fabricated by standard lithography and plasma etching. A 1-μm SiO_2 passivation layer was deposited by chemical vapor deposition. The Ohmic contacts with the p^+ and the n^+ layers were obtained by depositing 80×80 μm^2 Al contacts.

The QD formation and quality of the silicon layers was controlled *in situ* by RHEED (Fig. 2). The superstructure (2×1) characteristic of the atomically clean Si(001) surface is observed after the growth of the bottom *i*-Si region [Fig. 2(a)]. The oxidation gives rise to a change in the diffraction pattern. All the superstructure reflections disappear, and the bulk reflections become less intensive, while the diffusion background becomes more pronounced [Fig. 2(b)]. This implies the formation of a continuous oxide film on the silicon surface. Upon deposition of germanium on the oxidized silicon surface, a spotty RHEED pattern appears, exhibiting the same crystallographic orientations as the silicon substrate [Fig. 2(c)]. This indicates that the three-dimensional Ge islands were grown epitaxially with respect to the silicon surface.

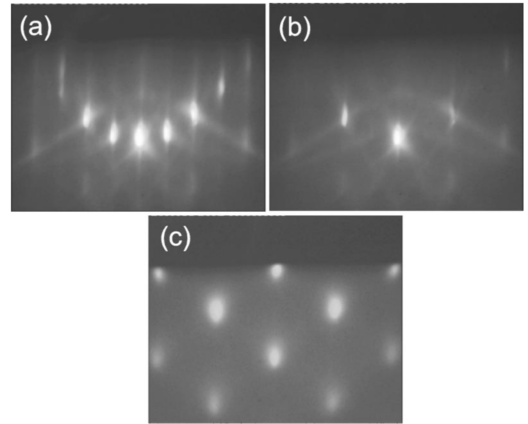

FIG. 2. RHEED patterns of the surface obtained after growth of the bottom *i*-Si region (a), after surface oxidation (b), and after 0.5-nm Ge deposition on silicon oxide (c).

The layer of QD's capped with a 10-nm-thick Si layer was examined with plan-view and cross-sectional electron microscopy using a transmission electron microscope CM20 FEG Philips with Gatan imaging filter GIF 200 (see Fig. 3). The Ge islands have a hemispherical shape with a base diameter of 5.8 ± 0.5 nm and a height of about 3–4 nm. The apex of the dots is oriented along the growth direction. The areal density of the islands was approximately 1.8×10^{12} cm^{-2}. To separate photoresponse from the dots, the reference sample was grown under conditions similar to the dot sample, except that no Ge was deposited.

It is necessary to note that when the nominal thickness of Ge layer reaches 1 nm, the distribution of Ge dot sizes becomes bimodal.[19] Along with the ultrasmall high-density islands, very large low-density ($\sim10^8$ cm^{-2}) lens-shaped Ge nanocrystals (≈200 nm in diameter and ≈40 nm in height) appear. However, as we will argue at the end of the paper, these islands do not contribute to the measured PC spectra.

PC measurements were performed in normal-incidence geometry (incident light polarized in the plane of the samples) at room temperature. Short-circuit (no bias) photocurrent was directly measured with a Keithley electrometer. For biased measurements, a lock-in amplifier was used. In the latter case, the light from globar source was mechanically chopped at the frequency of about 550 Hz. A low illumination power density of ~0.1 mW cm^{-2} was employed to provide an extremely low dot carrier occupancy and to avoid many-particle effects. In order to obtain the responsivity of the *p*-*i*-*n* diode, the spectral photon flux from the light

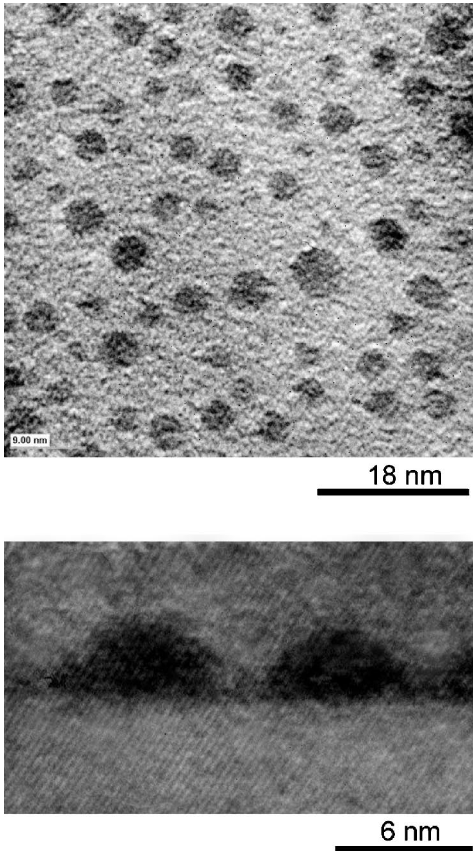

FIG. 3. Plan-view (top) and cross-section (bottom) transmission electron microscopy images of a dot sample. The Ge islands appear in dark contrast.

source was measured by using a calibrated pyroelectric detector.

III. RESULTS AND DISCUSSION

Figure 4 shows photocurrent spectra as a function of reverse bias. There is an apparent PC peak below the silicon interband absorption edge (1126 meV) which is not seen in the reference sample (crosses in Fig. 4). Since intra-valence-band-hole transitions in Ge/Si QD's occur at much lower energies[20] (70–400 meV), the observed photocurrent maximum cannot be attributed to the transition between hole states in the dots. At low bias, this peak has a symmetric line shape and is believed to come from the indirect excitonic transition between the hole ground state in the small Ge dots and the electron ground state confined in Si near the heterojunctions. The electron-hole pairs created by interband absorption thermally escape from the dots and give rise to the measured photocurrent. As the reverse bias increases, the current maximum becomes wider and splits into two peaks which are changed with the applied voltage in a different way. The position of the low-energy peak T_{low} is practically unchanged with the bias while the high-energy component T_{high} apparently shifts to *higher* energies.

To explain splitting and the blueshift of the high-energy transition, one needs to consider the electronic structure of

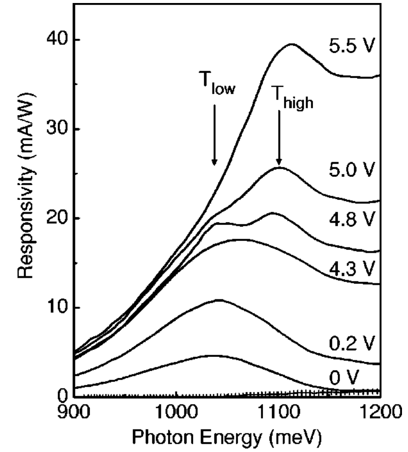

FIG. 4. Photocurrent spectra as a function of applied reverse bias (lines). The short-circuit photoresponse from a reference Si photodiode is shown by crosses.

excitons in type-II Ge/Si QD's. The modeling of the confined electron and hole states[11,12] predicts that holes are concentrated at the bottom of the dot, and the electrons are localized in Si both on top and below the Ge island. This is the result of strain distribution and Coulomb forces around the dot. Recently the confirmation of the spatial separation of electrons in the silicon matrix surrounding the Ge islands was provided by the observation of a negative interband photoconductivity in *n*-type Ge/Si(001) QDs.[21]

It follows from the second-order perturbation theory that the field dependence of the transition energy can be described by

$$E(F)=E(0)-eF(\langle z_h\rangle-\langle z_e\rangle)-\beta F^2, \qquad (1)$$

where $e=-|e|$ is the electron charge, $E(0)$ is the transition energy at zero field, $\langle z_{e,h}\rangle$ is the mean electron (hole) position along the growth direction (along the nanocrystal axis), and β is the polarizability of the electron-hole system.[2] In a system possessing an extremely large nonzero dipole moment, the second-order term in Eq. (1), quadratic in the applied field, may be less important than a linear one, and the transition energy is expected to vary linearly with the field.

In frame of this conception, we interpret the high-energy maximum T_{high} as a transition between the hole ground state in the Ge dot and the electron state confined in Si near the dot apex. The low-energy peak T_{low} is assigned to the transition between the same hole state and the electron state localized in Si near the dot base [see Fig. 1(b)]. Obviously, the term $eF(\langle z_h\rangle-\langle z_e\rangle)$ is negative for the first case and positive for the second one since the electron-hole dipoles formed as a result of the T_{high} and T_{low} transitions have the opposite directions.

We can check our explanation by extracting the values of electron-hole and electron-electron separation from the observed Stark shift. Keeping in mind that the observed PC maximum is a superposition of the two peaks, we decompose the maximum into two Gaussians. This allows us to determine the transition energies.[22] To extract the peak position at different bias from background photocurrent of Si band tail,

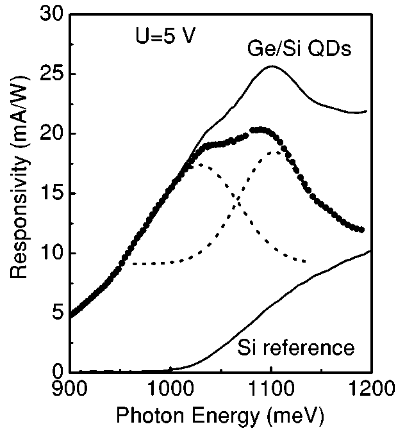

FIG. 5. Photocurrent spectrum at reverse bias 5 V. The response of a silicon *p-i-n* photodiode is given as a reference. Circles show the experimental data for the QD sample with the Si reference spectrum subtracted. Two dotted lines give the result of decomposition into two Gaussians. Fitting curve is shown by dash line.

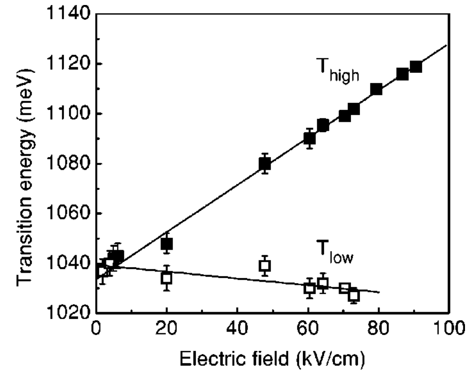

FIG. 6. Transition energies as a function of electric field. The solid lines are theoretical fits to the experimental data.

we measure the photoresponse spectra from the Si reference photodiode without QD's and subtract them from the QD sample spectra. An example of such subtraction and fitting is shown in Fig. 5 for reverse bias 5 V.

Then we performed a self-consistent one-dimensional simulation of our *p-i-n* device to calculate the electric field near the apex and the base of the dots. We used the model similar to that developed in Ref. 23. We found that electric field is uniform across the intrinsic region and can be well described by $F=(U+V_{bi})/W$, where U is the applied reverse bias, V_{bi} is the built-in potential (~ 1 V), and $W=0.8\ \mu$m is the intrinsic region width. Independent capacitance-voltage measurements carried out on the samples demonstrated that W does remain unchanged within the bias range studied and equal to the nominal growth width. This supports our calculation.

The field dependence of the transition energies is plotted in Fig. 6. As expected for a system with built-in dipole moments, the Stark shift for both transitions appears to be linear. Moreover, due to the linear behavior, the type-II Ge/Si QD's exhibit a QCSE of approximately one order of magnitude stronger than type-I InGaAs/GaAs QD's of similar height.[7] From a fit to the data using the Eq. (1), we find the electron-hole distance (5.1 ± 0.2) nm for the electron near the dot apex (top electron) and $-(0.8\pm 0.3)$ nm for the electron near the dot base (bottom electron). It is worth noting that separation of these two electrons (≈ 6 nm) is somewhat larger than the mean dot height (≈ 4 nm), which is quite reasonable for QD's with a staggered band lineup and provides clear support for the our explanation. The small separation of the bottom electron and the hole agrees with the fact that hole is localized towards the base of the dots.

The magnitude of the exciton polarizability is found to be $\beta/e^2=(120\pm 100)$ nm^2/eV for the $T_{\rm high}$ transition and $\beta/e^2=(1.5\pm 60)$ nm^2/eV for the $T_{\rm low}$ transition. The large error in the determination of β is consistent with the fact that the linear Stark shift is certainly dominated by the extremely large permanent exciton dipole. Since the polarizability is determined predominantly by the height of the quantum dots[2] and the spatial extent of the electrons wave functions above and below Ge QD's is close to the dot vertical dimension,[11] the polarizability values turn out to be comparable with those found for III-V dots of similar height.[2,3]

We now focus attention on the variation of the PC intensity with electric field. The amplitude of the low-energy signal increases with increasing F at low fields and saturates at bias $U\geqslant 5$ V. The intensity of the high-energy maximum continues to increase even at highest F. The increasing value of both PC peaks at low F can be related to an increasing rate of carrier escape with F. By applying a reverse bias, the electric field pushes the top electron towards the hole in the dot and pulls the bottom electron out from the hole. As a consequence, the electron-hole overlap and the corresponding absorption strength are increased for the $T_{\rm high}$ transition and reduced for the $T_{\rm low}$ transition. At highest F, no bound state can further exist for the bottom electron and the $T_{\rm low}$ transition transforms into a smooth PC tail on the low-energy side of the $T_{\rm high}$ signal.

Next let us discuss the possible role of huge Ge islands which are present in the structure due to the bimodal growth mode. We claim that these islands are of no importance for observed PC spectra due to the following arguments. First, the maximum external quantum efficiency η of the investigated photodiode deduced from the responsivity is about 1% at a telecommunication wavelength of 1.3 μm (at 953 meV). A similar value of η (2.3%) was achieved in Ge/Si quantum-dot waveguide photodetector, which contains five layers of Ge islands with a density of 3×10^9 cm^{-2} in each layer and was designed to have *a strong optical confinement*.[24] Obviously, one layer of Ge islands having a very low density (2×10^8 cm^{-2} for large islands in our samples) cannot ensure a measurable PC, especially at normal incidence. This is possible only for an extremely high-density QD structure. Second, 100-nm Ge/Si self-assembled islands usually exhibit an exciton related photoluminescence peak around ~ 800 meV (see Ref. 25 and references therein). To provide onset of interband transition at larger energies (1040–1100 meV), ultrasmall Ge QD's with enhanced size quantization of the hole energy spectrum are required.[26]

IV. SUMMARY AND CONCLUSIONS

The photocurrent spectroscopy of type-II Ge/Si(001) quantum dots, as a function of applied electric field, has demonstrated that the QD's possess two built-in electric dipoles of opposite orientations. We argue that this is a consequence of the spatial separation of the electrons around the dots. From the observed Stark shift, both separation of the electrons and hole at the dots and the distance between the electrons were determined. We found that, due to the linear behavior, the type-II Ge/Si QD's exhibit a QCSE of approximately one order of magnitude stronger than type-I InGaAs/GaAs QD's. An external quantum efficiency of about 1% at 1.3 μm of wavelength was obtained at room temperature. This result indicates that the Ge/Si QD's are potentially applicable for Si-based 1.3–1.5 μm optical fiber communication.

ACKNOWLEDGMENTS

The authors are much obliged to A. V. Nenashev for self-consistent calculations, N. P. Stepina for assistance in sample preparation, and I. B. Chistoknin for technical assistance. The work was supported by grants from the RFBR (Grant Nos. 03-02-16526 and 02-02-17746) and INTAS (Project Nos. 2001-0615 and 2001-0444).

---

*Electronic address: yakimov@isp.nsc.ru

[1] S.-S. Li, J.-B. Xia, J. Appl. Phys. **88**, 7171 (2000).

[2] J. A. Barker and E. P. O'Reilly, Phys. Rev. B **61**, 13 840 (2000).

[3] W. Sheng and J.-P. Leburton, Phys. Rev. Lett. **88**, 167401 (2002).

[4] K. L. Janssens, P. Partoens, and F. M. Peeters, Phys. Rev. B **65**, 233301 (2002).

[5] P. W. Fry, I. E. Itskevich, D. J. Mowbray, M. S. Skolnick, J. J. Finley, J. A. Barker, E. P. O'Reilly, L. R. Wilson, I. A. Larkin, P. A. Maksum, M. Hopkinson, M. Al'Khafaji, J. P. R. David, A. G. Cullis, G. Hill, and J. C. Clark, Phys. Rev. Lett. **84**, 733 (2000); P. W. Fry, I. E. Itskevich, S. R. Parnell, J. J. Finley, L. R. Wilson, K. L. Schumacher, D. J. Mowbray, M. S. Skolnick, M. Al-Khafaji, A. G. Cullis, M. Hopkinson, J. C. Clark, and G. Hill, Phys. Rev. B **62**, 16 784 (2000).

[6] A. Patanè, A. Levin, A. Polimeni, F. Schindler, P. C. Main, L. Eaves, and M. Henini, Appl. Phys. Lett. **77**, 2979 (2000).

[7] F. Findeis, M. Baier, E. Beham, A. Zrenner, and G. Abstreiter, Appl. Phys. Lett. **78**, 2958 (2001).

[8] Zhonghui Chen, Eui-Tae Kim, and Anupam Madhukar, Appl. Phys. Lett. **80**, 2770 (2002).

[9] A. Sacra, D. J. Norris, C. B. Murray, and M. G. Bawendi, J. Chem. Phys. **103**, 5236 (1995).

[10] V. Ya. Aleshkin, N. A. Bekin, N. G. Kalugin, Z. F. Krasil'nik, A. V. Novikov, V. V. Postnikov, and H. Seyringer, Pis'ma Zh. Éksp. Teor. Fiz. **67**, 46 (1998) [JETP Lett. **67**, 48 (1998)].

[11] A. I. Yakimov, N. P. Stepina, A. V. Dvurechenskii, A. I. Nikiforov, and A. V. Nenashev, Semicond. Sci. Technol. **15**, 1125 (2000); Phys. Rev. B **63**, 045 312 (2001).

[12] O. G. Schmidt, K. Eberl, and Y. Rau, Phys. Rev. B **62**, 16 715 (2000).

[13] M. A. Cusack, P. R. Briddon, S. M. North, M. R. Kitchin, and M. Jaros, Semicond. Sci. Technol. **16**, L81 (2001).

[14] M. Califano and P. Harrison, J. Appl. Phys. **91**, 389 (2002).

[15] J. M. Rorison, Phys. Rev. B **48**, 4643 (1993).

[16] O. P. Pchelyakov, Yu. B. Bolhovityanov, A. V. Dvurechenskii, A. I. Nikiforov, A. I. Yakimov, and B. Voigtländer, Thin Solid Films **362**, 75 (2000).

[17] A. A. Shklyaev, M. Shibata, and M. Ichikawa, Phys. Rev. B **62**, 1540 (2000); A. V. Kolobov, A. A. Shklyaev, H. Oyanagi, P. Fons, S. Yamasaki, and M. Ichikawa, Appl. Phys. Lett. **78**, 2563 (2001); A. A. Shklyaev and M. Ichikawa, *ibid.* **80**, 1432 (2002).

[18] A. Barski, M. Derivaz, J. L. Rouvière, and D. Buttard, Appl. Phys. Lett. **77**, 3541 (2000).

[19] A. G. Milekhin, A. I. Nikiforov, O. P. Pchelyakov, D. Tenne, M. Ladanov, S. Schulze, and D. R. T. Zahn, in *MRS 2002 Fall Meeting, Symposium E: Physics and Technology of Semiconductor Quantum Dots*, Boston, Mater. Res. Soc. Symp. Proc. **737**, E13.7.1 (2003).

[20] A. I. Yakimov, A. V. Dvurechenskii, Yu. Proskuryakov, A. I. Nikiforov, O. P. Pchelyakov, S. A. Teys, and A. K. Gutakovskii, Appl. Phys. Lett. **75**, 1413 (1999); A. I. Yakimov, A. V. Dvurechenskii, N. P. Stepina, and A. I. Nikiforov, Phys. Rev. B **62**, 9939 (2000); C. Miesner, O. Röthig, K. Brunner, and G. Abstreiter, Appl. Phys. Lett. **76**, 1027 (2000); C. Miesner, K. Brunner, and G. Abstreiter, Infrared Phys. Technol. **42**, 461 (2001); P. Boucaud, T. Brunhes, S. Sauvage, N. Yam, V. Le Thanh, D. Bouchier, N. Rappaport, and E. Finkman, Phys. Status Solidi B **224**, 233 (2001); T. Fromherz, W. Mac, A. Hesse, G. Bauer, C. Miesner, K. Brunner, and G. Abstreiter, Appl. Phys. Lett. **80**, 2093 (2002).

[21] A. I. Yakimov, A. V. Dvurechenskii, and A. I. Nikiforov, Pis'ma Zh. Éksp. Teor. Fiz. **73**, 598 (2001) [JETP Lett. **73**, 529 (2001)]; A. I. Yakimov, A. V. Dvurechenskii, N. P. Stepina, A. V. Nenashev, and N. I. Nikiforov, Nanotechnology **12**, 441 (2001).

[22] We find that this procedure works correctly for bias voltage less than 5.5 V. At larger voltage the only high-energy peak can be resolved unambigiously.

[23] P. N. Brunkov, S. G. Konnikov, V. M. Ustinov, A. E. Zhukov, A. Yu. Egorov, V. M. Maximov, N. N. Ledentsov, and P. S. Kop'ev, Fiz. Tekn. Poluprovodn. **30**, 924 (1996) [Semiconductors **30**, 492 (1996)]; P. N. Brunkov, A. Polimeni, S. T. Stoddart, M. Henini, L. Eaves, P. V. Main, A. R. Kovsh, Yu. G. Musikhin, and S. G. Konnikov, Appl. Phys. Lett. **73**, 1092 (1998).

[24] M. El kurdi, P. Boucaud, S. Sauvage, G. Fishman, O. Kermarrec, Y. Campidelli, D. Bensahel, G. Saint-Girons, I. Sagnes, and G. Patriarche, J. Appl. Phys. **92**, 1858 (2002).

[25] O. P. Pchelyakov, Yu. B. Bolhovityanov, A. V. Dvurechenskii, L. V. Sokolov, A. I. Nikiforov, A. I. Yakimov, and B. Voigtländer, Fiz. Tekn. Poluprovodn. **34**, 1281 (2000) [Semiconductors **34**, 1229 (2000)].

[26] C. S. Peng, Q. Huang, W. Q. Cheng, Z. M. Zhou, Y. H. Zhang, T. T. Sheng, and C. H. Tung, Phys. Rev. B **57**, 8805 (1998).